

## VIII-3 BROADBAND, FIXED TUNED, ACOUSTIC DELAY LINES AT L AND S BAND FREQUENCIES

L.R. Whicker, P.F. Garcia and G.E. Evans

Westinghouse

This paper is concerned with the design and development of broadband, fixed tuned, non-dispersive delay lines. These delay lines utilize multi-layer transducers incorporating CdS thin films of the type used by deKlerk<sup>1</sup>, sapphire delay media, and suitable electrical matching networks in either coaxial or strip transmission lines. The design of two broadband units are presented which operate at center frequencies of 1.80 GHz and exhibit 50 db bandwidths of approximately 50% with midband loss of approximately 40 db. The experimental data for these units are found to be in good agreement with theoretical values.

Before the specific designs of the two units are considered, the transducer impedance relationships are reviewed. The impedance is obtained by solving the piezoelectric equations subject to the boundary conditions shown in Figure 1. The impedance is given by<sup>2</sup>

$$Z = -\frac{jL}{\omega A\epsilon} + \frac{k^2 v}{\omega^2 A\epsilon} \left[ \frac{\frac{2\xi_0}{\xi_2} (1 - \frac{1}{\cos \beta L}) + j \tan \beta L}{1 + j \frac{\xi_0}{\xi_2} \tan \beta L} \right]$$
$$Z = R(\omega) - j X_c - j X(\omega).$$

This equation corresponds to the standard equivalent circuit of Figure 1b but is less convenient in that form. For many transducer configurations using CdS in the GHz range,  $R(\omega)$  may be as small as .01 ohm making possible only loose coupling from electromagnetic to acoustic energy. Correspondingly large mismatches are obtained (3000:1 for a 50-ohm line). Evans<sup>2</sup> has shown that this situation may be altered by adjusting the ratio  $\xi_0/\xi_2$ . Since  $\xi_2$  is the acoustic impedance seen looking into right electrode of Figure 1, various metallic layers may be used here to adjust the value of  $\xi_2$ . Figure 2 is a plot of values of  $R(\omega)$  and  $X(\omega)$  versus normalized frequency for various values of  $\xi_0/\xi_2$ .

The relationships of Figure 2 are useful in bandwidth considerations and indicate that a device having a large  $R(\omega)$  will of necessity, be a narrow band device. For cases in which  $\xi_2$  is obtained from multi-layer electrode arrangements, the ratio,  $\xi_0/\xi_2$ , will exhibit a frequency dependence and the relationships of Figure 2 will be modified.

In order to design broadband delay devices centered at 1.8 GHz, a computer program was prepared and several candidate multi-layer electrode configurations were investigated. Some of the more interesting designs are shown in Figure 3. In calculating these curves an additional series contact resistance,  $R_c$ , of value one ohm has been used. This resistance has been measured in physical configurations where spring like contacts are used in connecting the RF energy to the acoustic transducer electrode.

After evaluating the various transducer configurations, Design D of Figure 3 was selected as presenting the best electrical characteristics while offering ease of implementation. The physical transducer patterned after Design D is shown in Figure 4a. Here, thin combined layers of chromium and gold are used as the electrical electrodes while a 200 Å layer of SiO is included to insure isolation between the electrodes should pin holes be present in the CdS films. In this design, the CdS thickness was reduced due to resonator loading by the additional films. The attenuation characteristics for the overall transducer were calculated and found to be virtually the same as the original Design D. The diameters of the transducers were selected as .030 inches to provide the largest  $R(\omega)$  without adding significant diffraction loss when used in delay devices.

Two delay lines were designed and fabricated using the transducers of Figure 4a. The coaxial matching structure of Figure 4b was used in one device. Here two section Chebyshev transformers having characteristic impedances of 15.4 and 2.7 ohms are used for matching. The experimental attenuation and VSWR data for this device are given in Figure 5. The theoretical loss for two transducers also is included. It may be seen that the difference between the two curves can be accounted for by loss in the delay medium and in mismatch loss at the band edges. By incorporating a small absorber in the coaxial section of the device, the VSWR was reduced to below 2:1 over the bandwidth shown in the figure.

A second unit was designed in strip transmission line. In this design, three section Chebyshev matching transformers are utilized. In the matching sections, .030 and .010 inch ground plane spacings are used. A photograph of the partially assembled unit is shown in Figure 6. The attenuation data for this device are approximately the same as for the coaxial design while an improvement in VSWR is obtained (VSWR < 2:1 across 50% band).

In the paper, additional designs which operate at center frequencies of 450 and 850 MHz are discussed briefly. It is indicated that a total insertion loss of less than 13 db for 4  $\mu$ seconds of delay have been obtained over a 30% bandwidth for the 450 MHz device.

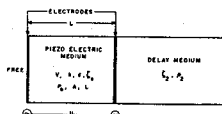
#### ACKNOWLEDGMENT

The authors are indebted to Dr. J. deKlerk for depositing the CdS films used in these experiments and to Mr. H. W. Cooper and Mr. D. D. O'Sullivan for their guidance and overall contributions to this program.

The work reported in this paper was sponsored in part by Harry Diamond Laboratories under Contract No. DAA 39-67-C-2042.

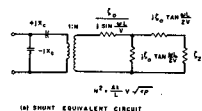
#### REFERENCES

1. J. deKlerk and E.F. Kelly, "Vapor Deposited Thin Film Piezoelectric Transducers," Rev. Scientific Instruments, Vol. 36, No. 4, 1965, p. 506.
2. G.E. Evans, "Fixed Tuned CdS Transducers," presented at 1966 Ultrasonic Symposium, Cleveland, Ohio, October 1966.



$V$  = VELOCITY OF SOUND  
 $A$  = AREA OF ELECTRODES  
 $\kappa$  = ELECTROMECHANICAL COUPLING COEFFICIENT  
 $\epsilon$  = DIELECTRIC CONSTANT  
 $\rho$  = ACOUSTIC IMPEDANCE +  $\rho V$   
 $\rho$  = DENSITY

(a) MODEL AND TERMS



(b) SHUNT EQUIVALENT CIRCUIT

FIG. 1 - Transducer Relationships

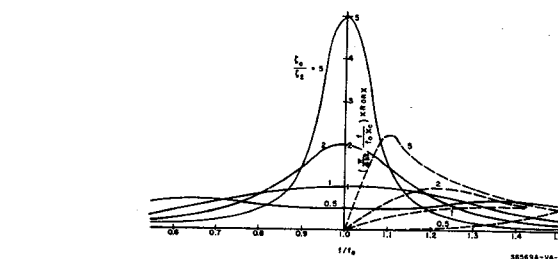
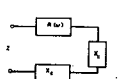
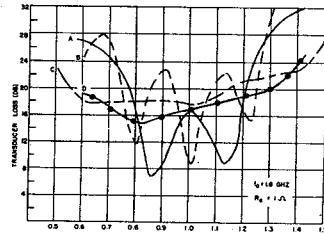


FIG. 2 -  $R(w)$  and  $X(w)$  Versus Normalized Frequency for Various  
for Various Values of  $\epsilon_0/\epsilon_2$



(2) BERLAKU EQUVALENT CIRCUIT



A	—	C	—
B	—	D	—
$\begin{array}{ c c c } \hline & \text{C5} & \text{W} & \text{Al}_2\text{O}_5 \\ \hline & \downarrow \frac{1}{2} & \downarrow \lambda & \downarrow \\ & \lambda & \lambda & \lambda \\ \hline \end{array}$		$\begin{array}{ c c c } \hline & \text{C5} & \text{W} & \text{Al}_2\text{O}_5 \\ \hline & \downarrow \frac{1}{2} & \downarrow \lambda & \downarrow \\ & \lambda & \lambda & \lambda \\ \hline \end{array}$	
$\begin{array}{ c c c } \hline & \text{C5} & \text{W} & \text{Al}_2\text{O}_5 \\ \hline & \downarrow \frac{1}{2} & \downarrow \frac{1}{2} & \downarrow \lambda \\ & \lambda & \lambda & \lambda \\ \hline \end{array}$		$\begin{array}{ c c c } \hline & \text{C5} & \text{W} & \text{Al}_2\text{O}_5 \\ \hline & \downarrow \frac{1}{2} & \downarrow \lambda & \downarrow \\ & \lambda & \lambda & \lambda \\ \hline \end{array}$	

FIG. 3 - Transducer Loss Versus Frequency

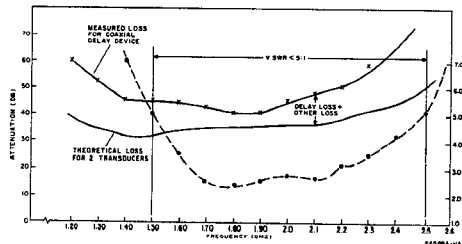


FIG. 5 - Theoretical and Experimental Data for Coaxial Delay Device

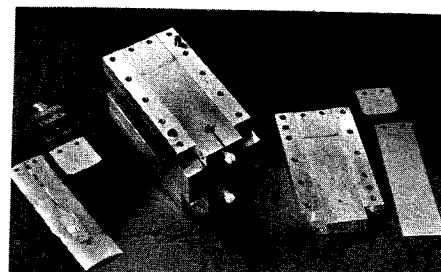


FIG. 6 - Photograph of Partially Assembled Ship Transmission Line Device

**MELABS**  
3300 Hillview Avenue, Stanford Industrial Park  
Palo Alto, California Telephone: 415-326-9500  
TWX: 910-373-1777

The latest in Ferrite Circulators, Isolators, Switches,  
Interdigital Filters, Mixers, Paramps, Sources.